Chitosan Nanoparticle Loaded with Quercetin and Valproic Acid: A Novel Approach for Enhancing Antioxidant Activity against Oxidative Stress in SH-SY5Y Cell Line

Fadime Canbolat *, Neslihan Demir, Ozlem Tonguc Yayıntas, Melek Pehlivan, Aslı Eldem, Tulay Kilicaslan Ayna, Mehmet Senel

Posted Date: 26 December 2023

doi: 10.20944/preprints202312.1970.v1

Keywords: antioxidant effect; chitosan; nanoparticle; oxidative stress; quercetin; valproic acid

Article

Chitosan Nanoparticle Loaded with Quercetin and Valproic Acid: A Novel Approach for Enhancing Antioxidant Activity against Oxidative Stress in SH-SY5Y Cell Line

Fadime Canbolat [1,*], Neslihan Demir [2], Ozlem Tonguc Yayıntas [3], Melek Pehlivan [4], Aslı Eldem [5], Tulay Kilicaslan Ayna [5,6] and Mehmet Senel [7,8]

[1] Çanakkale Onsekiz Mart University, Vocational School of Health Services, Department of Pharmacy Services, Çanakkale, Türkiye; fadime.canbolat@comu.edu.tr
[2] Çanakkale Onsekiz Mart University Faculty of Science, Çanakkale, Türkiye; neslihandemir@comu.edu.tr
[3] Çanakkale Onsekiz Mart University Faculty of Medicine, Çanakkale, Türkiye; oyayintas@comu.edu.tr
[4] İzmir Katip Çelebi University, Vocational School of Health Services, İzmir, Türkiye; pehlivanmlk@gmail.com
[5] İzmir Katip Çelebi University, Faculty of Medicine, Medical Biology Department, İzmir, Türkiye; aslierdem45@gmail.com, tulayayna@gmail.com
[6] İzmir Tepecik Education and Research Hospital, Tissue Typing Laboratory. İzmir, Türkiye; tulayayna@gmail.com
[7] Department of Biochemistry, Faculty of Pharmacy, Biruni University, Istanbul 34010, Türkiye; msenel81@gmail.com
[8] Department of Pharmaceutical Sciences, School of Pharmacy, University of California—Irvine, Irvine, California 92697, United States; msenel81@gmail.com
* Correspondence: fadime.canbolat@comu.edu.tr; +905304923303

Abstract: Background: Multiple drug delivery systems obtained by loading nanoparticles (NPs) with different drugs with different physicochemical properties present a promising strategy to achieve synergistic effects between drugs or overcome undesired effects. This study aims to develop a new NP by loading Quercetin (Que) and valproic acid (VPA) onto chitosan. In this context, our study investigated the antioxidant activities of chitosan NPs loaded with single and dual drugs containing Que against oxidative stress. Method: The synthesis of single (Que or VPA) and dual-drug (Que and VPA) loaded chitosan NPs, characterization of the NPs, conducting in vitro antioxidant activity studies, and analysis of the cytotoxicity and antioxidant activity of the NPs in SH-SY5Y cell lines were performed. Result: The NP applications that protected cell viability to the greatest extent against H2O2-induced cell damage were, respectively, 96 µg/ml of Que-loaded chitosan NP (77.30%, 48 h), 2 µg/ml of VPA-loaded chitosan NP (70.06%, 24 h), 96 µg/ml of blank chitosan NP (68.31%, 48 h), and 2 µg/ml of Que and VPA-loaded chitosan NP (66.03%, 24 h). Conclusion: Our study establishes a successful paradigm in developing drug-loaded NPs, with uniform and homogeneous distribution of drugs onto NPs. Chitosan NPs loaded with both single and dual drugs possessing antioxidant activity were successfully developed.

Keywords: antioxidant effect; chitosan; nanoparticle; oxidative stress; quercetin; valproic acid

1. Introduction

Valproic acid (2-n-propylpentanoic acid; VPA) is commonly prescribed for the treatment of migraine, bipolar disorder, epilepsy, and neuropathic pain [1,2]. In chronic use, the therapeutic concentration of VPA in plasma is typically 50-100 µg/ml for total VPA. However, VPA binds highly to albumin (approximately 95%), and as plasma concentration increases, the binding capacity to

 doi:10.20944/preprints202312.1970.v1

albumin becomes saturated, leading to an increase in free (unbound) VPA levels. Free VPA, responsible for the pharmacological effects of the drug, can also contribute to toxicity [3–5]. Although various therapeutic ranges for free VPA plasma concentration have been suggested (e.g., 5-15 or 7-23 μg/ml), an optimal range has not been established [4]. While the use of VPA at low doses is generally considered safe, serious side effects such as hepatotoxicity, pancreatitis, and hyperammonemia encephalopathy can occur at high doses [1,2,5]. The exact causes of these toxicities related to VPA use have not been fully elucidated; however, disruptions in mitochondrial and fatty acid mechanisms arising from VPA biotransformation, reactive metabolites, carnitine deficiency, and the formation of oxidative stress are associated with VPA toxicity [1]. Various studies on the formation of oxidative stress due to VPA use in epilepsy patients have reported high levels of malondialdehyde, a biomarker of oxidative stress. It has been suggested that the formation of oxidative stress may contribute to side effects such as pancreatitis and liver toxicity [1]. Drugs that can help reduce oxidative stress damage often contain flavonoid structures responsible for antioxidant activity. One of the most commonly used molecules in this group with antioxidant properties is Quercetin (Que). Que exhibits its antioxidant effect by scavenging reactive oxygen species (ROS) and chelating metal ions, thereby inhibiting the mechanism of lipid peroxidation [6]. The effective role of hydroxyl groups in the bioactivity of Que has been reported [6,7].

When examining the therapeutic efficacy of VPA and Que, various limitations in demonstrating the expected effects of these molecules emerge. These include VPA's high binding to plasma proteins, the formation of toxic metabolites, serious side effects at high doses, limited brain bioavailability of VPA crossing the blood-brain barrier (BBB) through anion transport proteins, and the strong antioxidant property of Que being hindered by rapid metabolism and low bioavailability. With today's technology, such limitations can be overcome through the development of nanoparticle (NP) formulations and the advancement of nanotechnological applications, including the addition of natural active substances for enhancing antioxidant activity and cellular protection. Chitosan, which holds a significant place in NP technology, is an FDA-approved, biologically degradable, biocompatible, and non-toxic polymer. Chitosan has demonstrated good antioxidant activity [6,7]. Literature reviews indicate the characterization studies of chitosan-VPA NPs [8]. These studies show promising drug activities characterized by NPs using lower VPA doses. NP applications can provide the expected response from the drug while simultaneously reducing drug toxicity by preventing the formation of toxic metabolites. Molecular structures, both endogenous and exogenous, that can participate in the antioxidant system help alleviate oxidative stress damage caused by drugs in organisms.

Multiple drug delivery systems obtained by loading NPs with different drugs with different physicochemical properties present a promising strategy to achieve potential synergistic effects between drugs or overcome undesired effects limiting the benefits of many potential drugs or compounds. This study aims to develop a new NP by loading Que and VPA onto chitosan. In this context, our study investigated the antioxidant activities of chitosan NPs loaded with single and dual drugs containing Que against oxidative stress. Accordingly, the synthesis of single (Que or VPA) and dual-drug (Que and VPA) loaded chitosan NPs, characterization of the synthesized NPs, conducting in vitro antioxidant activity studies, and analysis of the cytotoxicity and antioxidant activity of the synthesized NPs on human neuroblastoma SH-SY5Y cell lines were performed to achieve these objectives.

2. Materials and Methods

2.1. Standard and Reagents

Chitosan (deacetylation degree 95%), quercetin dihydrate, sodium tripolyphosphate (STPP), valproic acid (VPA), 1-ethyl-3-(3-dimethylaminopropyl)-carbodiimide hydrochloride and N-hydroxysuccinimide, 1,1- diphenyl-2-picrylhydrazyl (DPPH) and 2,2-azinobis (3-ethylbenzothiazoline-6-sulfonic acid) diammonium salt (ABTS) were purchased from Sigma-Aldrich (Darmstadt, Germany).

 doi:10.20944/preprints202312.1970.v1

2.2. Synthesis of Nanoparticles

The synthesis of the NPs in the study was carried out by modifying the methods of Zhang et al. 2008, Wang et al. 2020, Jardim et al. 2022, and Messias de Souza et al. 2022 [7,9–11]

2.2.1. Preparation of Blank Chitosan Nanoparticle (NP1)

Blank chitosan NP was synthesized by modifying the ionic chelation method in Zhang et al. 2008, Jardim et al. 2022 and Messias de Souza et al. 2022 [7,9,11]. For a 1 mg/mL chitosan solution, 100 mg chitosan was dissolved in 1.5% acetic acid solution. The pH of the solution was adjusted to 4.5 with 1 M sodium hydroxide solution. For a 1 mg/mL STPP solution, 100 mg STPP was dissolved in ultrapure water. The pH of the solution was adjusted to 4.5 by adding 10% hydrochloric acid. To 10 mL of chitosan solution (1 mg/mL pH: 4.5), 1 mg/mL STPP (pH: 4.5) was added dropwise for ionic chelation until the solution became turbid. The prepared sample was stirred at low speed on a magnetic stirrer for 24 hours.

2.2.2. Preparation of Quercetin-Loaded Chitosan Nanoparticle (NP2)

For 3 mg/mL Que solution, 33.5 mg quercetin dihydrate was weighed in a 10 mL flask and made up to volume with ethanol. The solution was kept in the darkness. To 10 mL of chitosan solution (1 mg/mL pH: 4.5), 1 mg/mL STPP (pH: 4.5) was added dropwise for ionic chelation until the solution became turbid. 1 mL Que solution (3 mg/mL) was added to the mixture. The prepared sample was stirred at low speed on a magnetic stirrer for 24 hours.

2.2.3. Preparation of Valproic Acid-Loaded Chitosan Nanoparticle (NP3)

The VPA and chitosan were conjugated by coupling carboxyl to amino group. Briefly, 2 mg/mL VPA was added to 10 mL of 1 mg/mL blank chitosan solution with 1 mL of 125 mM 1-ethyl-3-(3-dimethylaminopropyl)-carbodiimide hydrochloride and 1 mL of 125 mM N-hydroxysuccinimide. The prepared sample was mixed on a magnetic stirrer at low speed for 24 hours.

2.2.4. Preparation of Quercetin and Valproic Acid-Loaded Chitosan Nanoparticle (NP4)

2 mg/mL VPA and 1 mL of 3 mg/mL Que were added to 10 mL of 1 mg/mL blank chitosan solution with 1 mL of 125 mM 1-ethyl-3-(3-dimethyl aminopropyl)-carbodiimide hydrochloride and 1 ml of 125mM N-hydroxysuccinimide. The prepared sample was mixed on a magnetic stirrer at low speed for 24 hours.

After 24 hours of mixing, the samples were transferred to 50 mL falcon tubes and centrifuged at 8000 rpm for 40 minutes. After centrifugation of all NPs, the filtrates were stored at -20 °C to determine the amount of free drug. The residues were lyophilized at -47°C under 0.05 millibar for 24 hours and used for characterization, and antioxidant analyses. Samples were stored at -20°C.

2.3. Characterization Analysis of The Nanoparticles

2.3.1. Field Emission Scanning Electron Microscopy (FE-SEM) Analysis

The surface images were recorded by FE-SEM (JEOL JSM-7100F Schottky, the Netherlands). To increase the conductivity properties of the samples, firstly, an 8x10-1mbar/Pa vacuum was applied in the Quorum coating device, and 10 mA voltage was applied to the gold-palladium (80-20%) coating process. Photographs were taken by applying a voltage of 10 kV. Analyses were run in three replicates.

2.3.2. Transmission Electron Microscopy (TEM) Analysis

TEM analysis was performed using a JEOL JEM-1400 Plus 80 kV accelerating voltage. The samples were dispersed in water, and then, a 10 µL solution was deposited on a carbon-supporting

 doi:10.20944/preprints202312.1970.v1

grid. After solvent evaporation, the TEM analyses were performed. Analyses were run in three replicates.

2.3.3. Zeta analysis

The zeta potential characterization of the nanoparticles and the determination of the polydispersity index (PDI) were carried out using a Zetasizer Nano ZS instrument (ZEN 3600-Malvern Instruments, United Kingdom) at a temperature of 25°C. For the analysis, nanoparticles were dispersed in ultrapure water (approximately 0.01% by weight), sonicated for 10 minutes, and analyzed in triplicate at 25°C.

2.3.4. Fourier Transform Infrared Spectroscopy (FT-IR)

The samples' infrared spectra were recorded using an FT-IR Spectrum One (Perkin Elmer, USA) with the universal ATR sampling attachment (4000–450 cm−1) to examine the chemical structures. Analyses were run in three replicates.

2.3.5. Encapsulation Efficiency

NP suspensions were centrifuged at 7.000 g for 30 minutes. The free Que level in the supernatant at 415 nm (Queλmax) and the free VPA level at 302 nm (VPAλmax) were analyzed by UV-Vis spectrometer (Shimadzu Corporation, Kyoto, Japan). The encapsulation efficiency was determined using the efficiency calculation in Equation 1. Analyses were run in three replicates.

$$\text{Encapsulation efficiency (\%)} = (T\text{-}F)/T*100 \quad (1)$$

T: Total amount of Que and VPA in solution (μg/mL)
F: Amount of free Que and free VPA in the supernatant after centrifugation (μg/mL)

2.3.6. In Vitro Release Analysis

The kinetics of Que and VPA release were performed by adapting the methodology described by Jardim et al. [11]. For this purpose, approximately 1 mg of NPs were suspended with phosphate-buffered saline (PBS) at pH 7.4. Samples were kept under constant stirring (700 rpm) in a thermostated water bath at 37 ± 0.1 ºC. Each analysis was performed over 240 hours, with measurements taken at predetermined intervals. Supernatants were analyzed in a UV-Vis spectrometer. Analyses were performed in three replicates.

2.4. Antioxidant Activity Analysis

The concentration range of the standard and samples for antioxidant activity analysis was set at 0.05-0.6 mg/mL, and analyses were performed in three replicates. The DPPH radical scavenging activity of NPs was conducted following the method outlined by Blois et al. (1958) with slight modifications [12]. A 0.1 mM methanolic DPPH• solution was added to NP suspensions, and the mixture was incubated in the dark for 30 minutes at room temperature. Absorbance values of the reaction solutions were recorded at 517 nm, and butylated hydroxytoluene (BHT) was used as the standard. DPPH• radical scavenging activity was calculated using Equation 2.

The ABTS scavenging assay was performed as described by Re et al. (1999) [13]. ABTS•+ was generated by the oxidation of 7 mM ABTS with 2.45 mM potassium persulfate. Subsequently, the NP suspension was thoroughly mixed with the ABTS solution. After incubation in the dark for 15 minutes, the absorbance of the reaction mixture was recorded at 734 nm. The percentage scavenging of the ABTS•+ radical by the sample was calculated using Equation 2.

$$\text{\% scavenging activity} = [(Abs_{control} - Abs_{sample})/ Abs_{control}]*100 \quad (2)$$

Abssample is the absorbance of the sample, and Abscontrol is the absorbance of the blank solution.

 doi:10.20944/preprints202312.1970.v1

2.5. SH-SY5Y Cell Culture Conditions

The human neuroblastoma SH-SY5Y cell line was obtained from the American Type Culture Collection (CRL-2266™, ATCC, VA, USA). The cells were cultured in a nutrient mixture consisting of Dulbecco's Modified Eagle Medium (DMEM) (Gibco, Waltham, MA, USA) supplemented with 2mM L-glutamine, 100U/ml penicillin-streptomycin, and 10% heat-inactivated Fetal Bovine Serum (FBS), all obtained from Gibco (Gibco, Waltham, MA, USA). The culture was maintained in a humidified atmosphere at 37 °C with 5% CO2 according to the protocol outlined in the literature [14].

2.6. Nanoparticle Treatments and Cytotoxic Evaluation by MTT

The cytotoxic effect of the samples was assessed using the MTT (3-[4,5-dimethylthiazol-2-yl]-2,5-diphenyltratrazolium bromide) (BioFroxx, Germany) assay. In a 96-well plate, SH-SY5Y cells were seeded at 5x103 cells/well and allowed to attach to the surface for 24 h at 37 °C. The cells were exposed to 2 µg/ml, 8 µg/ ml, 24 µg/ml, 48 µg/ml, 72 µg/ml, and 96 µg/ml concentrations of each sample for 24 h and 48 h at 37 °C and incubated for 4 h by adding 5 mg/mL of MTT. As the final step, after removing the MTT solution, each well was filled with 100 ml of Dimethyl Sulfoxide (DMSO), and the plate was stored at 37°C for 10 min. Following the incubation period, cytotoxicity was determined spectrophotometrically at 570 nm by a microplate reader (Biotek™ Synergy™ HTX) [15]. The mean absorbance of the control cells was accepted as 100% viable. The effective dose (IC50) value was calculated. The percentage cell viability was calculated using Equation 3.

$$\% \text{ Cell viability} = (\text{Absorbance of cell treated cell})/(\text{Absorbance of cell control cell})*100 \quad (3)$$

2.7. Antioxidant Effect of Samples Against Hydrogen Peroxide-Induced Oxidative Stress in SH-SY5Y Cell Line

The cytotoxic effect of H2O2 in SH-SY5Y cells was determined through MTT analysis [15]. For MTT analysis, SH-SY5Y cells were seeded in a 96-well plate at a density of 5000 cells per well in a 10% DMEM medium. The cells were then incubated in a 37°C incubator with 5% CO2 for 24 hours. After 24 hours, the culture medium was removed from the wells, and the cells were exposed to 0 µg/ml, 2 µg/ml, 100 µg/ml, 200 µg/ml, 300 µg/ml, 500 µg/ml, and 1000 µg/ml concentrations of H2O2, which were then incubated for an additional 24 hours. Each concentration of H2O2 was tested in four replicate wells. At the end of the incubation period, the culture medium containing H2O2 was discarded, and 5 mg/mL of MTT solution was added to each well. The cells were further incubated for 4 hours. After incubation, the medium containing insoluble formazan crystals was removed, and the crystals were dissolved in 100 µl of DMSO. Absorbance at 570 nm was measured using a spectrophotometer. The viability of the H2O2 group was compared to the control group, where cell viability was considered 100%. The H2O2 dose that reduced cell viability by 50% (IC50; 200 µM) was determined, and oxidative stress was induced in SH-SY5Y cells. Subsequently, antioxidant activity analyses of NPs in SH-SY5Y cells were conducted. To evaluate the antioxidant effects of NPs, SH-SY5Y cells were exposed to 200 µM H2O2. The cells were initially seeded at a density of 5 × 103 cells/well in a 96-well plate and cultured overnight. Subsequently, 10 µL of NPs at various concentrations (2 µg/ml, 8 µg/ml, 24 µg/ml, 48 µg/ml, 72 µg/ml, and 96 µg/ml) was administered at 24 h and 48 h before treatment with 200 µM H2O2.

2.8. Statistical Evaluation

Logarithmic calculations were made from the dose-response graph GraphPad Prism 9 to obtain the IC50 values. Data were presented as the mean of triplicate experiments ± SD (****; p<0,0001,***; p<0,0005, **; p<0.005, *; p<0.05). Results were presented as mean (M) ± standard deviation (SD) of three replicate experiments. One-way ANOVA test was used to evaluate the differences between groups in antioxidant assays, and the post-hoc Tukey HSD test was used to compare groups.

 doi:10.20944/preprints202312.1970.v1

3. Results

When the FE-SEM and TEM images of the NPs developed by the ionic chelation method are examined in Figure 1 and Figure 2, it is seen that NP1 and NP3 are spherical in shape, while NP2 and NP4 have a strip-like structure.

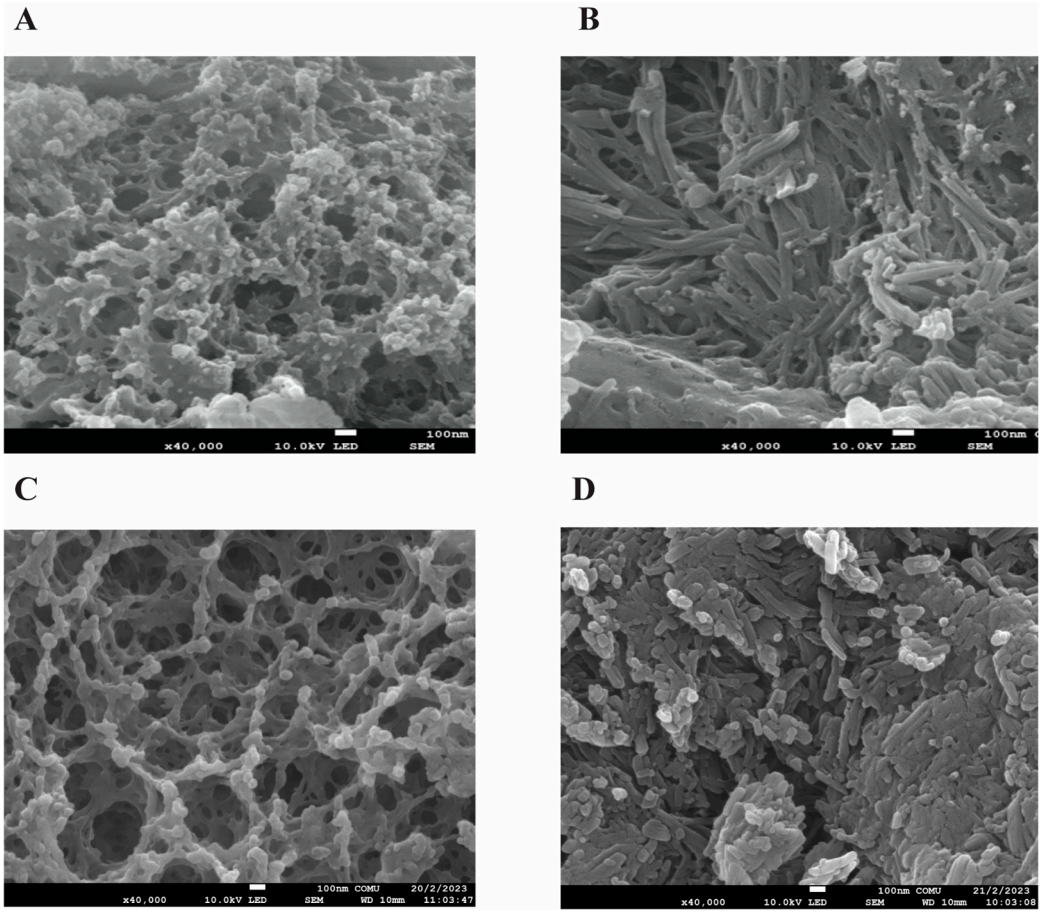

Figure 1. FE-SEM morphological evaluation of the nanoparticles (NPs). A) FE-SEM image of blank chitosan NP (NP1), B) FE-SEM image of Que-loaded chitosan NP (NP2), C) FE-SEM image of VPA-loaded chitosan NP (NP3), D) FE-SEM image of Que and VPA-loaded chitosan NP (NP4).

 doi:10.20944/preprints202312.1970.v1

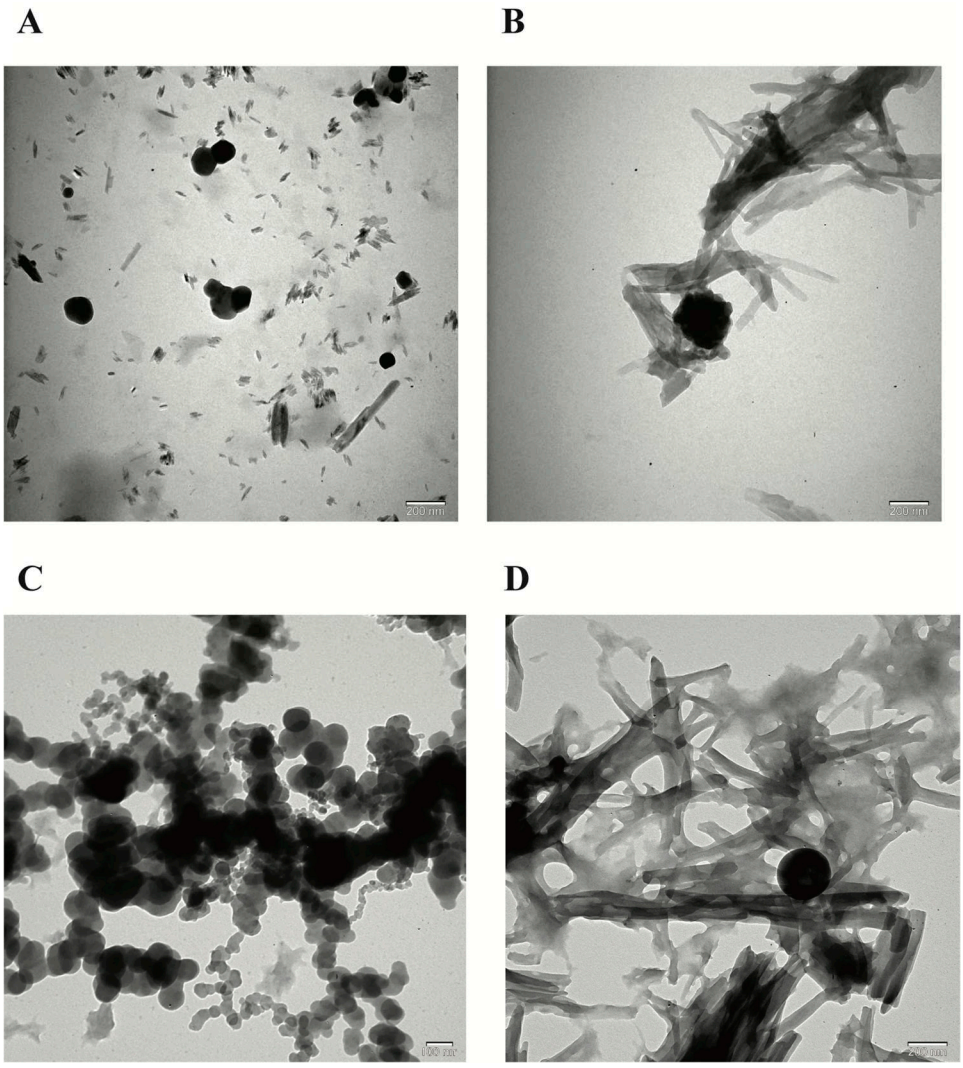

Figure 2. TEM morphological evaluation of the nanoparticles (NPs). A) TEM image of blank chitosan NP (NP1), B) TEM image of Que-loaded chitosan NP (NP2), C) TEM image of VPA-loaded chitosan NP (NP3), D) TEM image of Que and VPA-loaded chitosan NP (NP4).

Table 1 shows the NPs' particle size (nm) and zeta potential (mV) values according to TEM and Zeta analysis results. The mean particle size and zeta potential value of NP1, NP2, NP3, and NP4 were 153.6 ± 12.81 nm and 16.6 ± 4.12 mV, 180.5 ± 8.23 nm and 15.1 ± 3.42 mV, 93.2 ± 7.25 and 8.89 ± 3.82, 198.7 ± 9.13 and 27.2 ± 3.67 respectively. When examining the Zeta analysis results, the sharpness of the chromatograms, the zeta potential, and low PDI values indicate a stable and homogeneous distribution of the developed NPs within the solution. However, the stability of NP3 appears to be lower than the other NPs (Table 1, Figure 3).

Preprints (www.preprints.org) | NOT PEER-REVIEWED | Posted: 26 December 2023 doi:10.20944/preprints202312.1970.v1

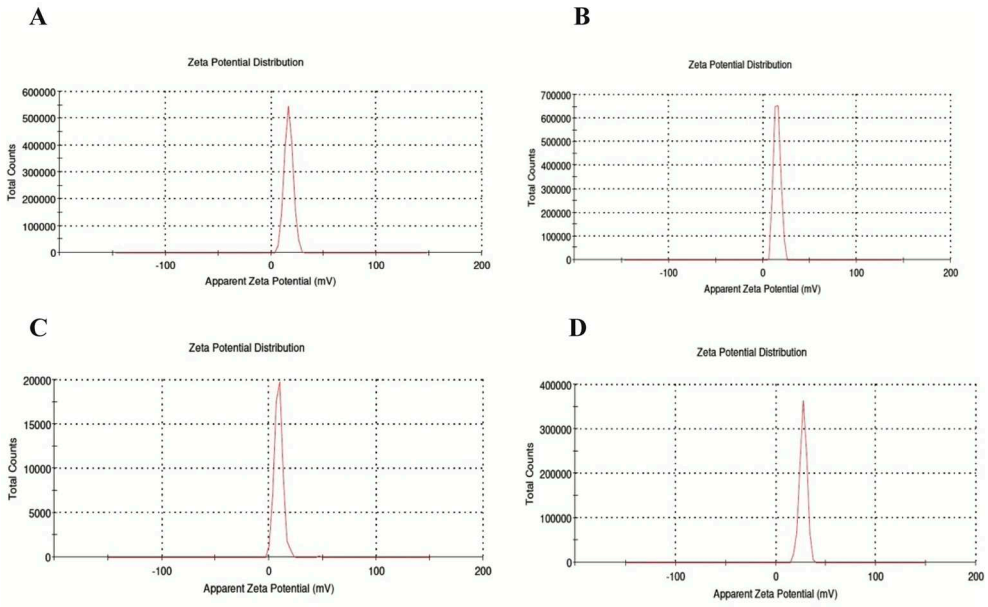

Figure 3. ZETA results of the developed nanoparticles (NPs) in the study. A) NP1; Blank chitosan NP, B) NP2; Que-loaded chitosan NP, C) NP3; VPA-loaded chitosan NP, D) NP4; Que and VPA-loaded chitosan NP.

The encapsulation efficiency of Que and VPA in the NPs has been determined to be above 95%, as calculated in Equation 1 (Table 1). Table 1 demonstrates a high encapsulation efficiency of Que and VPA loaded onto chitosan. Examination of the release of NPs at pH 7.4 and 37 ± 0.1°C indicated that Que exhibited a rapid release within the first 10 hours. In contrast, the burst release of VPA from chitosan NPs containing VPA commenced at the 50th hour in NP3 and at an earlier time, the 30th hour, in NP4 (Figure 4).

Table 1. Results of characterization analysis of nanoparticles.

Properties	NP1 (mean ± std. dev.)	NP2 (mean ± std. dev.)	NP3 (mean ± std. dev.)	NP4 (mean ± std. dev.)
Particle Size (nm)	153.6 ± 12.81	180.5 ± 8.23	93.2 ± 7.25	198.7 ± 9.13
Zeta Potential (mV)	16.6 ± 4.12	15.1 ± 3.42	8.89 ± 3.82	27.2 ± 3.67
PDI	0.08	0.05	0.08	0.05
Que level in total filtrate				
Que (µg/mL)	-	196.56 ± 7.65	-	23.49
Encapsulation Efficiency (%)	-	93.46 ± 5.52	-	99.23
VPA level in total filtrate				
VPA (µg/mL)	-	-	1.35	43.2
Encapsulation Efficiency (%)	-	-	99.9 ± 7.88	97.8± 5.42

NP1; Blank chitosan NP, NP2; Que-loaded chitosan NP, NP3; VPA-loaded chitosan NP, NP4; Que and VPA-loaded chitosan NP, PDI; polydispersity index, -; not detected.

The broad peak observed at 3313 cm^{-1} in the FT-IR spectrum of chitosan is due to the -OH and -NH stretching vibrations (Figure 4A). C-H bonds' symmetric and asymmetric stretching vibrations were observed at 2884 cm^{-1} (Figure 4A). The peaks observed around 1653 cm^{-1} indicate the presence of primary amine groups and N-H bending vibrations of amine-terminated chitosan [16]. The peak at 1027 cm^{-1} is due to the C–O stretching of the glucosamine ring, and the peak at 1545 cm^{-1} is ascribed to the N–H bending of the amino group [17]. Similar results were obtained in the FT-IR spectrum of

Preprints (www.preprints.org) | NOT PEER-REVIEWED | Posted: 26 December 2023 doi:10.20944/preprints202312.1970.v1

the synthesized NP1. In the FT-IR spectrum of Que, the broad peaks observed at 3414-3304 cm^{-1} correspond to O-H stretching vibration, while the peak observed at 1666 cm^{-1} corresponds to C=O aryl ketonic stretching vibration (Figure 4A). The 1518 cm^{-1} and 1613 cm^{-1} peaks correspond to C=C aromatic ring stretching vibrations. The peak at 1263 cm^{-1} corresponds to the C-O stretching vibration in the aryl ether ring, and the peak at 1324 cm^{-1} corresponds to the C-H stretching vibration of the aromatic ring [18]. Similar results were obtained in the FT-IR spectrum of NP2, and the C=O stretching vibration observed at 1664 cm^{-1} confirmed the presence of Que in chitosan (Figure 4A). Upon examination of Figure 4B, it is evident that both the VPA standard and the NPs containing VPA (NP3 and NP4) exhibit similar peaks at approximately 2961 cm^{-1} and 1700.6 cm^{-1}. In the FT-IR spectrum of VPA, the broad peaks observed at 2961.3 cm^{-1} indicate aliphatic O-H stretching vibration, while the peak at 1700.6 cm^{-1} corresponds to C=O stretching vibration [19,20]. Additionally, peaks attributed to Que, specifically the C=C aromatic ring, are observed at 1621 cm^{-1} and 1521 cm^{-1} in NP3 and NP4 (Figure 4B). This observation reveals that NPs can be appropriately developed.

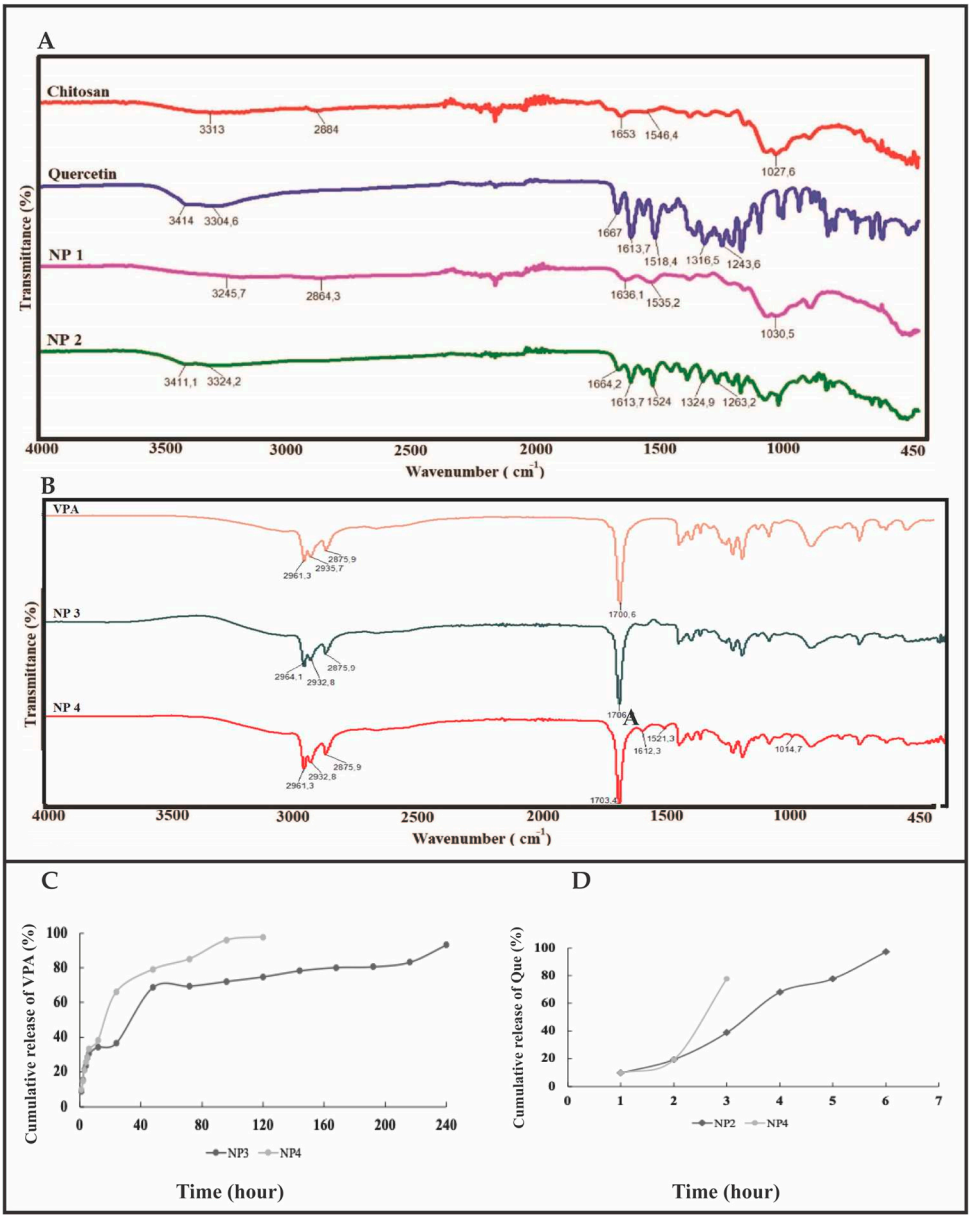

Figure 4. FT-IR and in vitro release analysis results. A) FT-IR analysis results of chitosan, Que, NP1, and NP2, B) FT-IR analysis results of VPA, NP1, and NP2, C) In vitro release analysis results of VPA, D) In vitro release analysis results of Que.

Preprints (www.preprints.org) | NOT PEER-REVIEWED | Posted: 26 December 2023 doi:10.20944/preprints202312.1970.v1

DPPH• and ABTS•+ radical scavenging activities are frequently used in studies investigating the antioxidant effect of Que-loaded NPs. In our study, the antioxidant activity of NPs was determined using these methods. Each NP's antioxidant activity within the dose range of 0.05-0.6 mg/mL was compared with the standard antioxidant activity of BHT. The analysis data are depicted in Figure 5. In the DPPH and ABTS analysis results, the antioxidant activity of NP1 and NP3, which do not contain Que, was found to be lower compared to the antioxidant activity of BHT at all concentrations. A statistically significant difference was found between BHT, NP1, and NP3 antioxidant activity results in both antioxidant activity analyses ($p < 0.05$). In the DPPH analysis result, the antioxidant activity of NP2 and NP4, which contain Que, was comparable to or higher than the antioxidant activity of BHT. Antioxidant activity increased dose-dependently. The antioxidant activity of BHT varies between 49.77% and 90.84%, while the antioxidant activity of NP2 appears to range from 74.67% to 88.33%, and NP4's antioxidant activity is observed to be between 63.19% and 90.15%.

In DPPH analysis, the antioxidant activity of NP2 was higher than that of BHT at 0.05, 0.1, and 0.2 mg/mL levels, while it was close to the activity of BHT at 0.4, and 0.6 mg/mL levels. The antioxidant activity of NP4 was higher than that of BHT at 0.05, and 0.1 mg/mL levels, while it was close to the activity of BHT at 0.2, 0.4, and 0.6 mg/mL levels. NP2 showed the highest DPPH scavenging activity at 0.4 mg/mL, and NP4 showed the highest DPPH scavenging activity at 0.6 mg/mL (Figure 5A).

In the ABTS analysis results, although the antioxidant activity of NP2 and NP4 was lower than that of BHT, a dose-dependent antioxidant activity was observed, similar to the BHT standard regarding antioxidant effect. NP2 and NP4 showed the highest ABTS•+ radical scavenging activity at 0.6 mg/mL concentration (83.21 ± 4.91 and 77.70 ± 7.27, respectively). When the antioxidant analysis data were examined, it was found that NP2 and NP4 containing Que exhibited antioxidant activity close to BHT, while NP1 and NP3 were the NPs with the lowest antioxidant activity (Figure 5B).

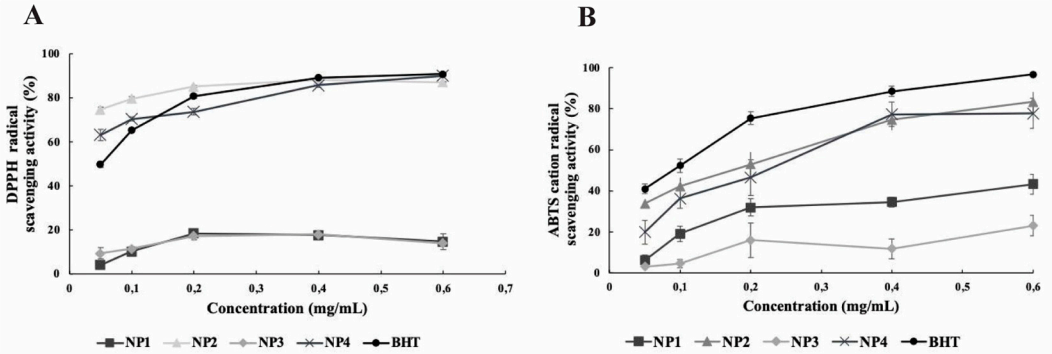

Figure 5. Results of in vitro antioxidant activity of the nanoparticles (NPs). NP1; Blank chitosan NP, NP2; Que-loaded chitosan NP, NP3; VPA-loaded chitosan NP, NP4; Que and VPA-loaded chitosan NP, A) DPPH activity analysis, B) ABTS activity analysis.

To evaluate the cytotoxicity and antioxidant effect of the synthesized NPs on human neuroblastoma SH-SY5Y cell lines, the H_2O_2 value to be applied to the cells was determined. As a result of the MTT test, IC_{50} value was determined as 200 μM (Figure 6).

Preprints (www.preprints.org) | NOT PEER-REVIEWED | Posted: 26 December 2023 doi:10.20944/preprints202312.1970.v1

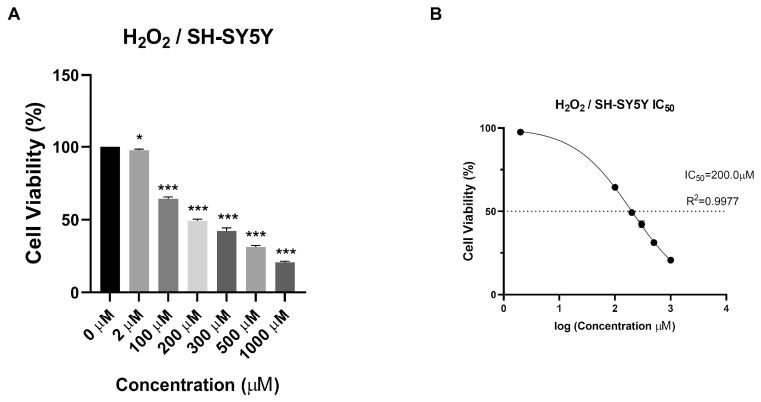

Figure 6. The cytotoxic effect of H2O2 with different concentrations (0 µg/ml, 2 µg/ml, 100 µg/ml, 200 µg/ml, 300 µg/ ml, 500 µg/ ml, 1000 µg/ ml) on SH-SY5Y cells at 24th. A) % cell viability of SH-SY5Y cells treated with H2O2 at different concentrations for 24h. B) The IC50 values of H2O2 for 24h. Experiments were carried out in triplicate. Data are expressed as mean ± standard deviation (S.D.). *p<0.05, ***<0.001.

Que and VPA-loaded chitosan NPs were applied to SH-SY5Y cells at different doses, and cell cytotoxicity was evaluated. Except for high doses of NP4, none of the samples showed cytotoxic effects at the concentrations used in the study. At the concentration of 96 µg/mL applied to the cells, NP4 was observed to reduce cell viability by approximately 50% at 24 h (Figure 7), and by around 40% at 48 h (Figure 8).

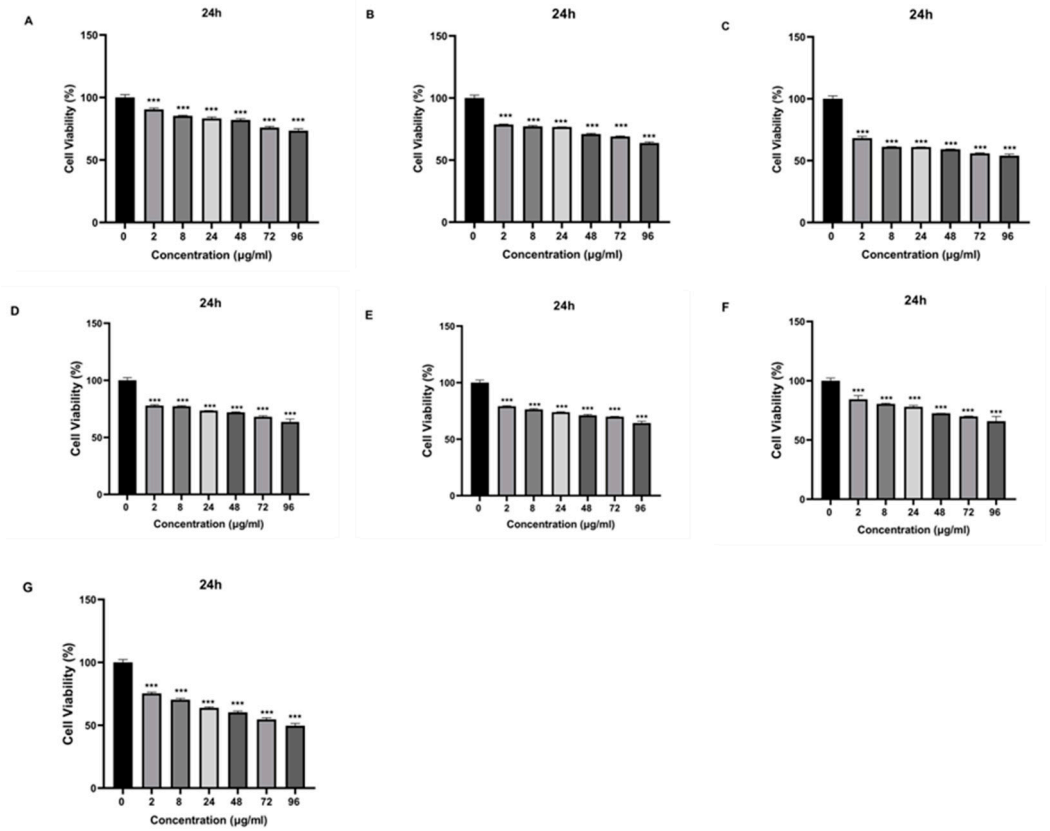

Figure 7. The cytotoxic effect of samples with different concentrations (0 µg/ml, 2 µg/ml, 8 µg/ml, 24 µg/ml, 48 µg/ml, 72 µg/ml, and 96 µg/ml) on SH-SY5Y cells at 24th h. A) VPA, B) Que, C) Chitosan, D) NP1, E) NP2, F) NP3, G) NP4. Experiments were carried out in triplicate. Data are expressed as mean±standard deviation (S.D.). ***p<0.001.

Preprints (www.preprints.org) | NOT PEER-REVIEWED | Posted: 26 December 2023 doi:10.20944/preprints202312.1970.v1

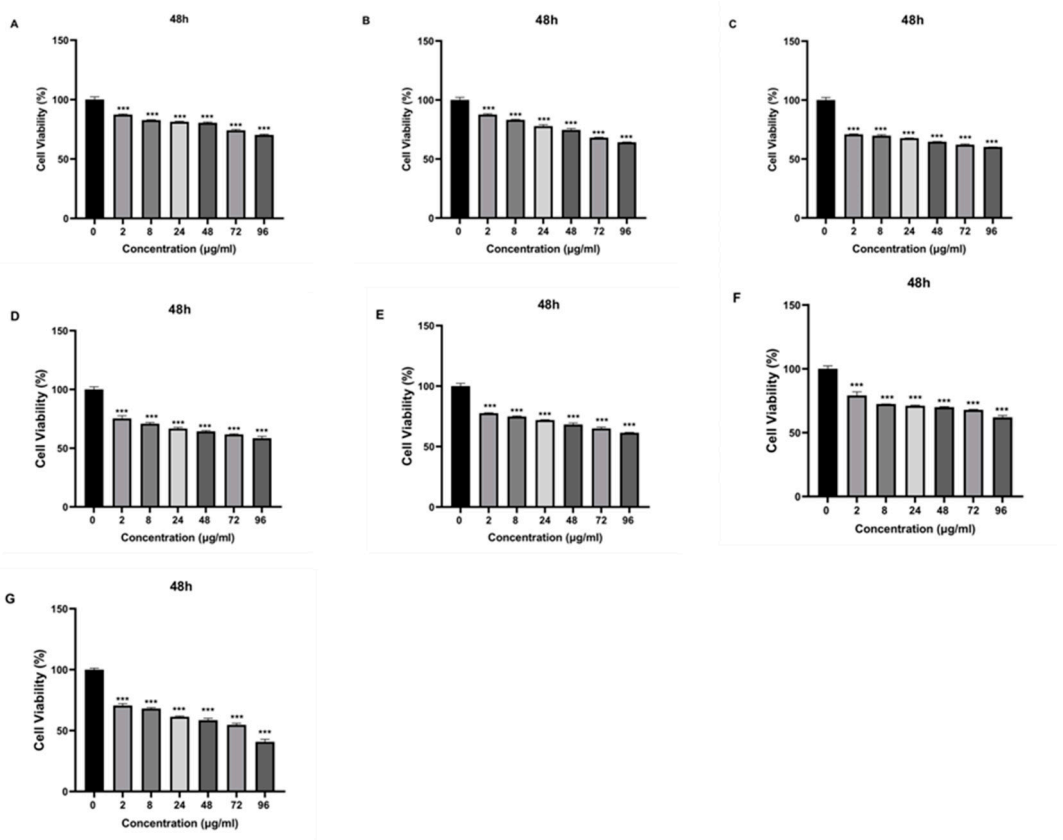

Figure 8. The cytotoxic effect of samples with different concentrations (0 µg/ml, 2 µg/ml, 8 µg/ml, 24 µg/ml, 48 µg/ml, 72 µg/ml, and 96 µg/ml) on SH-SY5Y cells at 48th h. A) VPA, B) Que, C) Chitosan, D) NP1, E) NP2, F) NP3, G) NP4. Experiments were carried out in triplicate. Data are expressed as mean±standard deviation (S.D.). ***p<0.001.

To assess the antioxidant potential of NPs against oxidative stress, SH-SY5Y cells were subjected to pretreatment with different concentrations of NPs for 24 h and 48 h, followed by exposure to 200 µM H2O2 for 24 h. While 50% cell viability was observed in SH-SY5Y cells treated solely with H2O2, cell viability increased when cells were pretreated with NPs before exposure to H2O2. Additionally, it has been observed that when VPA, Que, and chitosan molecules present in the composition of NPs are applied to SH-SY5Y cells exposed to hypoxia at different concentrations (2 µg/ml, 8 µg/ml, 24 µg/ml, 48 µg/ml, 72 µg/ml, and 96 µg/ml), these molecules exhibit antioxidant activity, thereby exerting a protective effect on cell viability (Figure 9, Figure 10).

Preprints (www.preprints.org) | NOT PEER-REVIEWED | Posted: 26 December 2023 doi:10.20944/preprints202312.1970.v1

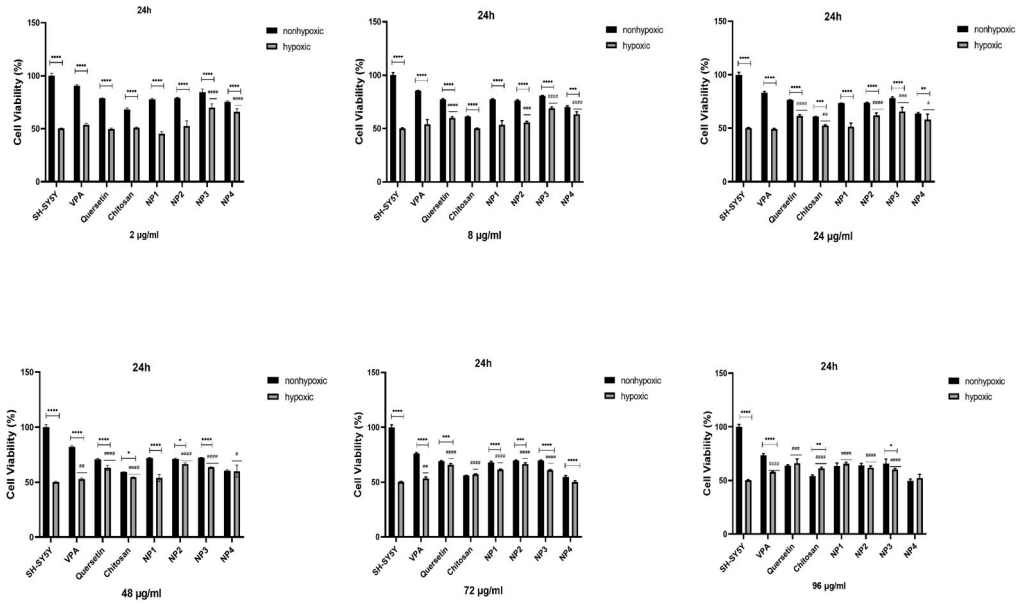

Figure 9. The antioxidant effect of samples with different concentrations (2 µg/ml, 8 µg/ml, 24 µg/ml, 48 µg/ml, 72 µg/ml, and 96 µg/ml) on H2O2-challenged SH-SY5Y cells for 24th h. Experiments were carried out in triplicate. Data are expressed as mean ± standard deviation (S.D.). Compared to hypoxic vs nonhypoxic groups ****; p<0.0001,***; p<0.0005, **; p<0.005, *; p<0.05, Compared to nonhypoxic SH-SY5Y vs sample hypoxic groups ####; p<0.0001, ###; p<0.0001, ##; p<0.005, #; p<0.05.

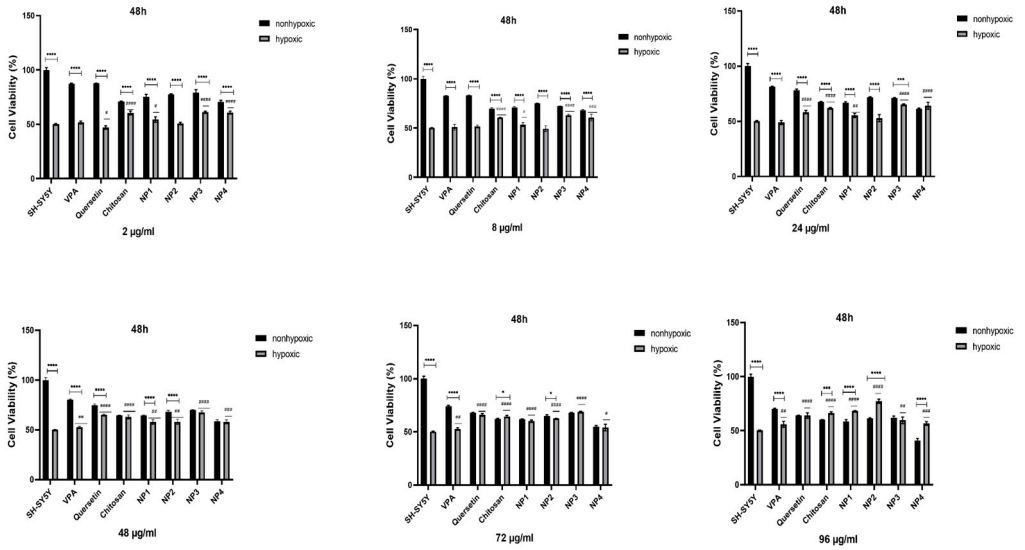

Figure 10. The antioxidant effect of samples with different concentrations (2 µg/ml, 8 µg/ml, 24 µg/ml, 48 µg/ml, 72 µg/ml, and 96 µg/ml) on H2O2-challenged SH-SY5Y Cells for 48th h. Experiments were carried out in triplicate. Data are expressed as mean ± standard deviation (S.D.). Compared to hypoxic vs nonhypoxic groups ****; p<0.0001,***; p<0.0005, **; p<0.005, *; p<0.05, Compared to nonhypoxic SH-SY5Y vs sample hypoxic groups ####; p<0.0001, ###; p<0.0001, ##; p<0.005, #; p<0.05.

When 48 µg/ml, 72 µg/ml, and 96 µg/ml of VPA were applied to the cells, it was determined that cell viability increased at 24 h and 48 h. With the increase in dose, cell viability was significantly elevated ($p < 0.01$). At 24 h, the increase in dose resulted in a cell viability range of 52.77% to 57.89% (Figure 9), while at 48 h, the increase in dose led to a cell viability range of 52.7% to 55.83% ($p < 0.01$) (Figure 10). The highest efficacy was achieved at 24 h by applying 96 µg/ml VPA, resulting in 57.89%

 doi:10.20944/preprints202312.1970.v1

cell viability ($p < 0.0001$). However, it was observed that low and moderate doses of VPA (2 μg/ml, 8 μg/ml, and 24 μg/ml) did not have a significant impact on cell viability ($p > 0.05$) (Figure 9).

When Que was applied to the cells at different doses during both intervals, the lowest dose did not show a noticeable effect on cell viability. In 24 h, the cell viability was 49.95% in cells treated with 2 μg/ml of Que, and this rate decreased to 47.06% at 48 h ($p< 0.05$), resulting in a significant difference compared to the control group. However, the application of 8 μg/ml Que began to demonstrate efficacy by increasing cell viability by 59.8% at 24 h ($p < 0.0001$) (Figure 9). At the same time, no significant effect was observed at this dose at 48 h (Figure 10). It was observed that the application of 24 μg/ml, 48 μg/ml, 72 μg/ml, and 96 μg/ml Que significantly increased cell viability with dose increment at both 24 h and 48 h. At 24 h, cell viability increased by 61.3% to 66.0% with dose increment, while at 48 h, cell viability increased by 58.32% to 65.99% with dose increment ($p < 0.0001$). The highest efficacy was achieved by applying 96 μg/ml Que at 24 h, resulting in 66.0% cell viability ($p < 0.0001$).

When chitosan was applied to the cells at different doses, it was observed that low doses of chitosan (2 μg/ml and 8 μg/ml) did not significantly increase cell viability at 24 h ($p > 0.05$) (Figure 9). However, at 48 h, these low doses significantly increased cell viability, reaching approximately 60% ($p < 0.0001$) (Figure 10). It was determined that the application of 24 μg/ml, 48 μg/ml, 72 μg/ml, and 96 μg/ml of chitosan significantly increased cell viability with dose escalation at both 24 h and 48 h. At 24 h, cell viability increased in the range of 52.54% to 61.04% with dose escalation, while at 48 h, cell viability increased in the range of 62.12% to 66.31% with dose escalation ($p < 0.0001$). The highest efficacy was achieved by applying 96 μg/ml chitosan at 48 hours ($p < 0.0001$).

When NP1 was applied to the cells at different doses, it was observed that the low and moderate doses of NP1 (2 μg/ml, 8 μg/ml, 24 μg/ml, and 48 μg/ml) did not significantly increase cell viability at 24 h ($p > 0.05$) (Figure 9). However, at 48 h, these doses were found to significantly increase cell viability ($p < 0.01$, $p < 0.05$) (Figure 10). NP1 treatment exhibited a protective effect at concentrations of 72 μg/ml and 96 μg/ml against H2O2 toxicity at both time points (24 h and 48 h) ($p < 0.0001$). It was determined that applying 72 μg/ml NP1 at 24 h and 48 h increased cell viability to approximately 60% ($p < 0.0001$). Additionally, the application of 96 μg/ml NP1 at 24 h and 48 h elevated cell viability to above 65%, with the highest efficacy observed at 48 h with 96 μg/ml NP1, reaching 68% cell viability ($p < 0.0001$).

Upon application of NP2 at different doses to the cells, it was observed that, at 24 hours, only the low dose (2 μg/ml) did not significantly increase cell viability ($p > 0.05$) (Figure 9). However, at 48 hours, it was observed that low and moderate doses (2 μg/ml, 8 μg/ml, and 24 μg/ml) did not significantly increase cell viability ($p > 0.05$) (Figure 10). When NP2 levels of 8 μg/ml, 24 μg/ml, 48 μg/ml, 72 μg/ml, and 96 μg/ml were applied to the cells for 24 h, a significant increase in cell viability by 55.49% to 66.53% was observed ($p < 0.0001$). The highest efficacy was achieved by applying 48 μg/ml NP2 at 24 h ($p < 0.0001$). However, when NP2 levels of 48 μg/ml, 72 μg/ml, and 96 μg/ml were applied to the cells for 48 h, a significant increase in cell viability by 60.38% to 77.30% was observed ($p < 0.0001$). NP2 demonstrated a protective effect against H2O2-induced cytotoxicity at all doses, with a more pronounced effect at higher doses. Particularly at 96 μg/ml, it exhibited a 77.30% protective effect against H2O2-induced cytotoxicity.

In NP3 applications, cell viability remained above 60% for all dose applications at both time points (24 h and 48 h). However, in the 24th h cell viability analysis, the cell viability ratio was significantly high for all doses (60.24-70.06%), and as the dose increased, the increase in cell viability decreased (Figure 9). As shown in Figure 9, NP3 demonstrated the highest antioxidant effect when applied at 2 μg/ml, maintaining cell viability up to 70%.

In the 24th h application, it was observed that the low and moderate doses of NP4 (2 μg/ml, 8 μg/ml, 24 μg/ml, and 48 μg/ml) significantly increased cell viability up to 66% (Figure 9). In the 24 h pre-treatment experiment, NP4 at 72 μg/ml, and 96 μg/ml provided lower protection against neurotoxicity (Figure 9). In contrast, 2 and 8 μg/ml NP4 preserved cell viability up to 66.03% and 63.18%, against H2O2, respectively. NP4 exhibited the highest viability at a concentration of 2 μg/ml at 24 h. In other words, the dose with the best protective effect for NP4 was 2 μg/ml at 24 hours. In

 doi:10.20944/preprints202312.1970.v1

the 48 h pre-treatment experiment, the low, moderate, and high doses (2 µg/ml, 8 µg/ml, 24 µg/ml, 48 µg/ml, 72 µg/ml, and 96 µg/ml) were observed to significantly increase cell viability in the range of 54.13% to 64.09% for all doses (Figure 10). The efficiency of 48 µg/ml, 72 µg/ml, and 96 µg/ml NP4 was lower, whereas 2 µg/ml, 8 µg/ml, and 24 µg/ml NP4 protected cell viability up to 60.78%, 60.63%, and 64.09% against H2O2, respectively.

In cell culture analyses, it has been observed that all NPs increased cell viability against H2O2-induced cell damage (Figure 11).

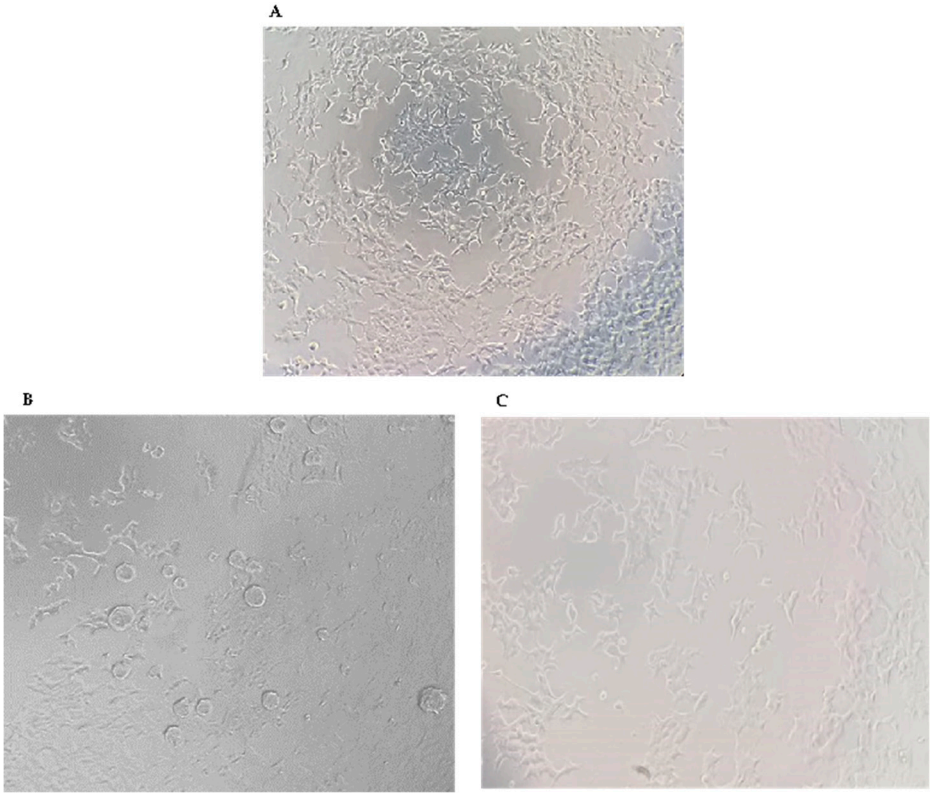

Figure 11. Images of cell viability of SH-SY5Y cells are included in the study. A) untreated SH-SY5Y, B) H2O2-induced damage in SH-SY5Y Cell, C) NPs exposure to H2O2-induced damage in SH-SY5Y Cell.

4. Discussion

The synthesis of the NPs in this study was carried out by modifying the methods of Zhang et al 2008, Wang et al 2020, Jardim et al 2022, and Messias de Souza et al 2022 [7,9–11]. The preparation of chitosan NPs is based on an ionic gelation interaction between positively charged chitosan and negatively charged STPP at room temperature. The chitosan NPs prepared in the experiment were in white powder, similar to the literature [7,9–11]. Que stock solution was prepared in ethanol as in the literature [7,9,11]. NP1 and NP3 were white, while NP2 and NP4 were yellowish, indicating that the Que was loaded into the chitosan. In synthesizing NPs, pH, ultrasonic bath soaking time, stirring speed, and duration were considered. In our study, when FE-SEM (Figure 1) and TEM (Figure 2) images are examined, it is seen that NP1 and NP3 are nearly spherical shape [21], and NP2 and NP4 are strip-like structures [22]. The FE-SEM and TEM images of the NPs synthesized in our study exhibit similarities with the images of NPs containing Que and VPA in the literature [22–26]. Images and zeta potential values of NPs kept in an ultrasonic bath at pH 4.5 for 5 minutes and stirring at low speed for 24 hours are given in Table 1 and Figure 3.

The mean particle size and zeta potential value of NP1 and NP2 were 153.6 ± 12.81 nm and 16.6 ± 4.12 mV, 180.5 ± 8.23 nm and 15.1 ± 3.42 mV, respectively (Table 1). The positive zeta potential of NP substrate assisted suitable interaction and ionic cross-linking of NPs to negatively charged molecules. This clearly shows that the loading of Que on chitosan NPs causes a significant decrease

 doi:10.20944/preprints202312.1970.v1

in the zeta potential. A similar situation was also reported in the Roy and Rhim study (2021) [6]. Li et al. 2018 performed single and double-molecule loadings to chitosan. In the study, the particle size of Que loaded on chitosan NP was found to be 190.7 ± 2.8 nm [26]. The particle size of the NPs obtained in our study is similar to the literature. In our study, NP1 and NP3 were formulated with a mean diameter of 153.6 ± 12.81nm and 93.2 ± 7.25 nm, for both chitosan and VPA-loaded chitosan samples, respectively (Table 1). The loading of VPA into chitosan led to a decrease in size by about 60 nm. The results may be attributed to the electrostatic interaction and ionic cross-linking between negatively charged VPA and positively charged chitosan molecules, which have led to electric attraction force among substrates and final shrinkage of the particles. A similar situation to our study is also observed in the study conducted by Jafarimanesh et al [23]. In their 2023 study, Jafarimanesh et al developed chitosan NPs loaded with VPA. When the particle sizes of the synthesized NPs in Jafarimanesh et al.'s study were examined, a decrease in particle size was observed with VPA loading. In our study, in NP4, where dual drug loading occurred, the NP size increased upon adding Que. Therefore, the data from our study demonstrates similarity with the literature. The biochemical influence of scaffolds is a key factor in their applicability, and great attention is required for the particle surface characteristics and particle size distribution. The magnitude of the zeta potential provides information about particle stability [23]. To evaluate the stability of the synthesized NPs, zeta potential measurements were used. Higher magnitude potentials indicate increased electrostatic repulsion and, thus, increased stability. Particles with zeta potentials in the 0-5 mV range tend to aggregate or cluster, particles in the 5-20 mV range are stable, and particles above 20 mV are highly stable [27]. When the zeta potential data in Table 1 and Figure 3 are examined, it is seen that the zeta potential values of NP1, NP2, and NP3 are in the range of 5-20 mV and can show a stable structure. The NP with the highest zeta potential and exhibiting high stability in our study was identified as NP4. The proximity of the PDI values of all developed NPs to zero in our study indicates a homogeneous nanoparticle distribution (Table 1). This observation suggests that each NP exhibits similar sizes, and their distributions are not widely spread. In addition, the sharpness of the zeta potential peak in Figure 3 provides information about the homogeneity of the structure. When examining the Zeta analysis results, the sharpness of the chromatograms and the potential values indicate a stable and homogeneous distribution of the developed NPs within the solution. All obtained results indicate that drugs were homogeneously loaded onto NPs, and this loading was uniformly distributed. This situation may support the effectiveness of drug transport, enabling the drug to reach the targeted area more efficiently. Thus, it suggests a potential contribution to enhancing the bioavailability of the drugs.

FT-IR spectroscopy revealed that both spectra of Que standard and NP2 have the same characteristic peaks of O-H (3400 cm-1) and aromatic C=C (1510 cm-1, 1610 cm-1). Still, the intensity of the sample peaks is lower (Figure 4A). The peaks at 3411.1 cm-1, 1613.7 cm-1, and 1515.6 cm-1 appearing in the FT-IR analysis of the Que standard are observed at approximate values in NP2. The peaks at 1653 cm-1 and 1022 cm-1 appearing in the FT-IR analysis of the chitosan standard are also seen at approximate values in NP1 and NP2. In the Roy and Rhim study, 1614 cm-1 was noted as the prominent peak of Que [6]. This observation reveals that NPs can be developed appropriately, as our data are similar to other studies in the literature [6,24,26,28]. Upon examination of Figure 4B, it is evident that both the VPA standard and the NPs containing VPA (NP3 and NP4) exhibit similar peaks at approximately 2961 cm-1 and 1700.6 cm-1. In the FT-IR spectrum of VPA, the broad peaks observed at 2961.3 cm-1 indicate aliphatic O-H stretching vibration, while the peak at 1700.6 cm-1 corresponds to C=O stretching vibration [19,20]. Additionally, peaks attributed to Que, specifically the C=C aromatic ring, are observed at 1621 cm-1 and 1521 cm-1 in NP3 and NP4. This observation reveals that nanoparticles can be appropriately developed.

Encapsulation efficiency is a crucial factor in drug delivery release. For the sustained release of an adequate amount of the drug at the target site, a high level of entrapment of the drug into the NPs is expected [11]. The encapsulation efficiency of Que NPs developed with different methods in the literature was obtained as 79.8 ± 1.5% [29], 83.8 ±0.33% [11], and 92% [30]. In our study, when the amounts of drugs in the filtrates were analyzed for encapsulation efficiency, it was observed that due

to the trace amounts of drugs in the filtrates, drug loading in the NPs was achieved with high encapsulation efficiency. In our study, Que encapsulation efficiency was found to be 93.46 ± 5.52% and 99.23 ± 4.73% in NP2 and NP4, respectively. In our study, VPA encapsulation efficiency was found to be 99.9 ± 7.88% and 97.8± 5.42% in NP3 and NP4, respectively (Table 1). In our study, NPs with higher encapsulation efficiency were synthesized compared to the literature. The reasons for this include that adjusting the optimal solvent, pH, stirring speed, and time during synthesis effectively develops NPs.

The results showed that VPA and Que release profiles from chitosan NPs were rapid in our study. In the study conducted by Jafarimanesh et al. in 2023, VPA was loaded onto chitosan NPs within a hybrid of alginate/chitosan hydrogel. The study observed a rapid release of VPA from the chitosan hydrogel loaded with VPA, with the initial burst release of VPA observed after 72 hours of incubation [23]. In our study, the burst release of VPA from chitosan nanoparticles containing VPA started at the 50th hour in NP3 and at an earlier time, the 30th hour, in NP4 (Figure 4C). Raj et al. 2015 reported that the release of Que was rapid in the first 10 hours [25]. In our study, when the release of NPs at pH 7.4 37 ±0.1°C was examined, it was observed that Que was rapidly within the first 8 hours (Figure 4D). The data of our study are similar to the literature.

Due to the antioxidant properties of Que, Que-loaded NPs have been developed using different nanostructures in the literature. When the antioxidant activities of NPs in the literature are examined, Li et al. 2018 reported that genipin and Que-loaded chitosan NPs showed antioxidant activity in DPPH and ABTS assays [26]. Wu et al. (2008) reported that NPs composed of Que, polyvinyl alcohol, and aminoalkyl methacrylate copolymers showed antioxidant activity in vitro [31]. Zhang et al (2008) studied the radical removal activity of Que-loaded chitosan NPs in the 0.5-3 mg/mL range. As a result of the analysis, it was reported that the NP showed antioxidant activity [32]. Unlike Zhang et al.'s (2008) study, the radical scavenging activity and antioxidant capacity of NPs at lower concentrations were investigated in our study. In our study, antioxidant activity analysis of samples in the range of 0.05-0.6 mg/mL was performed. In our study, determining the antioxidant capacities of the NPs developed against ROS was among our research objectives. To achieve this, in vitro antioxidant capacity analyses were conducted to determine the effectiveness of the NPs. In our study, the antioxidant activity capacity of NPs containing Que was observed to be close to the antioxidant activity capacity of the BHT standard (Figure 5). Effective antioxidant activity was observed in NP2 and NP4. However, NP1 and NP3 without Que showed significantly lower antioxidant activity than the BHT standard (Figure 5). In a study conducted by Palol et al. (2021), the antioxidant activity of VPA was evaluated using the DPPH analysis method [33]. Compared to ascorbic acid, the antioxidant activity of VPA was found to be approximately 35%, exhibiting lower antioxidant capacity than ascorbic acid. In our study, it was observed that NP3, which contains only VPA, exhibited low antioxidant activity. However, NP4, which underwent dual drug loading by adding Que, showed antioxidant activity close to the BHT standard. Our study results are consistent with similar findings in the literature. The analysis results indicate that the antioxidant property of Que can be successfully utilized in NP systems, and this property of Que persists within the NP system.

Additionally, in our study, the antioxidant activity of the developed NPs was analyzed on hypoxia-induced SH-SY5Y cells, selected for evaluating neurotoxicity processes. H2O2 is commonly used as an inducer of oxidative stress in in vitro models. As a result of the MTT test, IC50 value was determined as 200 μM (Figure 6). Additionally, the potential cytotoxic effects of free VPA, Que, chitosan, and NPs were determined after 24 h (Figure 7) and 48 h (Figure 8). Except for high doses of NP4, none of the samples showed significant cytotoxic effects at the concentrations used in the study (Figure 7, Figure 8). At the concentration of 96 μg/mL applied to the cells, NP4 was observed to reduce cell viability to below 50%. When reviewing studies examining the cytotoxic effects of VPA, Que, and chitosan in SH-SY5Y cells, it was observed in a study by Suematsu et al. (2011) that Que did not demonstrate any significant cytotoxic effect in the range of 0–100 μM [34]. Manigandan et al. (2019) reported that chitosan did not show any significant cytotoxic effect at levels between 0 and 50 μM [35], while Terzioglu Bebitoglu et al. (2020) found that VPA at concentrations of 1 mM, 5 mM, or 10 mM did not exhibit any cytotoxic effect on SH-SY5Y cells [36]. In our study, antioxidant effects were

 doi:10.20944/preprints202312.1970.v1

explored in a model of H2O2-induced oxidative stress in SH-SY5Y cells. The mechanism of H2O2-induced cell damage includes the production of reactive hydroxyl radicals and byproducts by Fenton's reaction that further interact directly with cellular components to damage proteins, lipids, and DNA [37]. Antioxidants can block these effects. Cell viability was measured 24 h and 48 h after H2O2-induced damage. Suematsu et al. (2011) examined the protective effects of Que against the death of H2O2-treated SH-SY5Y cells [34]. When SH-SY5Y cells were incubated in a medium containing 100 μM H2O2 and Que, H2O2-mediated damage was suppressed. When SH-SY5Y cells were cultured with 100 μM H2O2, cell viability decreased to approximately 38% of the vehicle-treated cells. In the presence of Que, the viability of H2O2-treated cells increased in a Que concentration-dependent manner, reaching about 67% of that of the vehicle-treated ones at 100 μM Que [34]. Xi et al. (2012) studied the protective effects of Que in H2O2-induced SH-SY5Y cells [38]. SH-SY5Y cells were pre-cultured with Que in different concentrations for 12 h or 10 μM for various periods, then pre-conditioned cells were treated with H2O2 (0.5 mM, 12 h). The study revealed that Que arrested cellular damage. In the 2018 study by Han et al., the antioxidant effect of Que-loaded NP was analyzed in SH-SY5Y cells [39]. The DCFH-DA fluorescent probe was selected to determine the total intracellular ROS level, and 200 μM H2O2 was used as a positive control in the study. Que powders could reduce amounts of ROS products to some extent, as indicated by most of the studies. When Que NPs were introduced, the ROS level was neutralized, similar to the cell control, indicating that Que NPs exhibit a unique ROS scavenging activity. Cell viability increased from 40% to 70% with 10 μg/mL of Que NPs [39]. Similar to the literature, in our study, a hypoxic environment was created by applying 200 μM H2O2 to SH-SY5Y cells (Figure 6). In our study, the antioxidant activity of free Que and NP2-containing Que became apparent starting from 8 μg/mL after 24 h (Figure 9). The highest efficacy was achieved by applying 96 μg/mL Que and 48 μg/mL NP2 at 24 h, resulting in approximately 66.0% cell viability ($p < 0.0001$) (Figure 9). Additionally, it was observed that the antioxidant activity of free Que and Que-containing NP2 was initiated at 24 μg/mL for free Que and 48 μg/mL for NP2 after 48 h of application (Figure 10). The highest efficacy was achieved by applying 72 μg/mL Que (65.99% cell viability) and 96 μg/mL NP2 at 48 hours, resulting in 77.30% cell viability ($p < 0.0001$) (Figure 10). Our study demonstrates a similarity to the literature regarding the antioxidant effect of Que on H2O2-induced SH-SY5Y cells.

All NPs developed in our study were synthesized using chitosan. Publications indicate that chitosan positively enhances cell viability in H2O2-induced SH-SY5Y cells. In a study conducted by Manigandan et al. (2019), applying 5-20 μM chitosan to H2O2-induced SH-SY5Y cells was reported to increase cell viability by approximately 70% [35]. Similarly, in our study, it was observed that both free chitosan and all NPs developed using chitosan increased cell viability in hypoxic cells. The application of 24 μg/mL, 48 μg/mL, 72 μg/mL, and 96 μg/mL chitosan significantly increased cell viability in a dose-dependent manner at both 24 h and 48 h. Within 24 h, cell viability increased between 52.54% and 61.04% in a dose-dependent manner (Figure 9), and within 48 h, cell viability increased between 62.12% and 66.31% in a dose-dependent manner ($p < 0.0001$) (Figure 10). The highest efficacy was achieved with the application of 96 μg/mL chitosan at 48 h, reaching 70% cell viability ($p < 0.0001$) (Figure 10). The application of NP1 (blank chitosan NP) showed a protective effect against H2O2 toxicity at concentrations of 72 μg/mL and 96 μg/mL ($p < 0.0001$). Applying 96 μg/mL NP1 for 24 h and 48 h raised cell viability to over 65%, with the highest efficacy observed at 48 h with 96 μg/mL NP1, resulting in 68% cell viability ($p < 0.0001$). Similar to the findings in the literature, the results of our study also indicate a positive effect of chitosan on cell viability. This suggests the potential for a synergistic effect in antioxidant activity within NPs developed with chitosan, owing to its protective impact.

In a study conducted by Terzioglu Bebitoglu et al. (2020), SH-SY5Y human neuroblastoma cells were pre-treated with 1 mM, 5 mM, or 10 mM VPA and then compared with 15 mM glutamate exposure [36]. The MTT test was applied to determine cell viability, and the treatment with 1 mM VPA effectively increased the viability of cells exposed to glutamate for 24 h. In our study, the effect of free VPA as well as single and dual drug-loaded NPs on cell viability after H2O2 treatment was investigated. When cells were treated with 48 μg/ml, 72 μg/ml, and 96 μg/ml VPA, an increase in cell

 doi:10.20944/preprints202312.1970.v1

viability was observed at 24 h and 48 h. Moreover, an evident increase in cell viability was observed with dose escalation ($p < 0.01$). The highest efficacy was achieved by applying 96 μg/ml VPA at 24 h, reaching 57.89% cell viability ($p < 0.0001$). However, no significant effect on cell viability was observed with low and medium doses of VPA (2 μg/ml, 8 μg/ml, and 24 μg/ml) ($p > 0.05$). The positive effect of VPA on cell viability in our study is consistent with the literature. In NP3 applications, cell viability remained above 60% in all dose applications at both time points (24 h and 48 h). NP3 exhibited the highest neuroprotective effect when applied at 2 μg/ml, maintaining cell viability up to 70%. While free VPA does not exhibit antioxidant activity at low doses, it is observed that NP3 (chitosan-loaded VPA NP) shows antioxidant activity even at low doses. This suggests a synergistic effect of chitosan and VPA molecules in the NP3 content contributing to antioxidant activity.

In the 24 h application experiment, low and medium doses of NP4 (2 μg/ml, 8 μg/ml, 24 μg/ml, and 48 μg/ml) significantly increased cell viability up to 66% (Figure 9). In the 24-h pre-treatment experiment, NP4 provided lower protection against neurotoxicity at concentrations of 72 μg/ml, and 96 μg/ml (Figure 9). In other words, the optimal dose for the best antioxidant effect of NP4 was determined to be 2 μg/ml at 24 h. In the 48 h pre-treatment experiment, low, medium, and high doses (2 μg/ml, 8 μg/ml, 24 μg/ml, 48 μg/ml, 72 μg/ml, and 96 μg/ml) significantly increased cell viability between 54.13% and 60.78% (Figure 10). The efficiency of 48 μg/ml, 72 μg/ml, and 96 μg/ml NP4 was lower, whereas 2 μg/ml, 8 μg/ml, and 24 μg/ml NP4 protected cell viability up to 60.78%, 60.63%, and 64.09% against H_2O_2, respectively. In our study, free VPA demonstrated antioxidant effects at high doses, while when used in conjunction with chitosan and Que within NPs, it could exhibit antioxidant effects at lower doses. This indicates that combining bioactive molecule contents in nanoparticle formulations can achieve antioxidant effects at lower doses. However, the inability of NP4 to demonstrate antioxidant effects at high doses is thought to be related to the cytotoxicity analysis of NP4, where high doses may reduce the cell viability of healthy cells (Figure 7, Figure 8).

This study's findings demonstrate the in vitro antioxidant activities of the developed NPs and their protective effects in the H_2O_2-induced oxidative stress model. In vitro antioxidant capacity analyses have revealed that Que-containing NPs, especially NP2 and NP4, exhibit activity close to the antioxidant activity capacity of the BHT standard (Figure 5). While the antioxidant activity of NP1 and NP3 without Que was found to be lower compared to the antioxidant activity of BHT (Figure 5), all developed NPs were observed to protect against H_2O_2-induced cell damage and exhibit protective effects against oxidative stress in cell culture experiments (Figure 9, Figure 10).

In cell culture experiments, the protective effects of NPs on SH-SY5Y cells were assessed. NP applications that provided the highest protection against H_2O_2-induced cell damage (Figure 11), respectively, were determined as follows: NP2 at 96 μg/ml (77.30%, 48 hours), NP3 at 2 μg/ml (70.06%, 24 hours), NP1 at 96 μg/ml (68.31%, 48 hours), and NP4 at 2 μg/ml (66.03%, 24 hours). Our study emphasizes the positive effects of chitosan on antioxidant activity. NP1, which contains chitosan, demonstrated a protective effect, especially at high doses, against H_2O_2 toxicity. Furthermore, the low doses of NP3 and NP4, containing valproic acid, exhibiting antioxidant activity in SH-SY5Y cells exposed to oxidative damage, suggest a potential novel therapeutic approach against oxidative injury during VPA treatment. Additionally, it was observed that NP2 and NP4, containing Que, exhibited a significant protective effect against oxidative stress induced by H_2O_2. Despite the cytotoxicity observed at high doses of NP4, its antioxidant effect persisted at low doses. This suggests that NP4 has a notable protective potential at appropriate doses, while higher doses may adversely affect cell viability. When evaluating studies in the literature regarding the effective use of drug-loaded NPs in brain diseases [40] and considering our analysis results, it is believed that NPs developed by loading onto chitosan may potentially play a role in alleviating oxidative stress associated with neurodegenerative conditions.

5. Conclusions

Our study establishes a successful paradigm in developing drug-loaded NPs, with uniform and homogeneous distribution of drugs onto NPs. This optimized drug loading pattern not only ensures efficient drug. In our study, chitosan NPs loaded with both single and dual drugs possessing

antioxidant activity were successfully developed. The NPs created through the combination of Que, VPA, and chitosan, especially at optimized doses, emerge as promising therapeutic agents capable of alleviating oxidative stress associated with neurodegenerative conditions in our study. These findings underscore the importance of single and dual drug loadings in nanotechnology for developing new and effective strategies to reduce oxidative stress during the pharmacological treatment of neurological diseases.

Supplementary Materials: The following supporting information can be downloaded at the website of this paper posted on Preprints.org, Figure S1. FE-SEM morphological evaluation of the nanoparticles (NPs); Figure S2. TEM morphological evaluation of the nanoparticles (NPs); Figure S3. ZETA results of the developed the nanoparticles (NPs) in the study; Figure S4. FT-IR and in vitro release analysis results; Figure S5. Results of in vitro antioxidant activity of the nanoparticles (NPs); Figure S6. The cytotoxic effect of H2O2 with different concentrations (0 µg/ml, 2 µg/ml, 100 µg/ml, 200 µg/ml, 300 µg/ ml, 500 µg/ ml, 1000 µg/ ml) on SH-SY5Y cells at 24th.; Figure S7. The cytotoxic effect of samples with different concentrations (0 µg/ml, 2 µg/ml, 8 µg/ml, 24 µg/ml, 48 µg/ml, 72 µg/ml, and 96 µg/ml) on SH-SY5Y cells at 24th h.; Figure S8.The cytotoxic effect of samples with different concentrations (0 µg/ml, 2 µg/ml, 8 µg/ml, 24 µg/ml, 48 µg/ml, 72 µg/ml, and 96 µg/ml) on SH-SY5Y cells at 48th h. ; Figure S9. The antioxidant effect of samples with different concentrations (2 µg/ml, 8 µg/ml, 24 µg/ml, 48 µg/ml, 72 µg/ml, and 96 µg/ml) on H2O2-challenged SH-SY5Y cells for 24th h.; Figure S10. The antioxidant effect of samples with different concentrations (2 µg/ml, 8 µg/ml, 24 µg/ml, 48 µg/ml, 72 µg/ml, and 96 µg/ml) on H2O2-challenged SH-SY5Y cells for 48th h.; Figure S11. Images of cell viability of SH-SY5Y cells are included in the study; Table S1. Results of characterization analysis of the nanoparticles

Author Contributions: F.C. is the first author of this study. Conceptualization, F.C. and M.S.; methodology, all authors; validation, F.C., N.D., M.P. and T.K.A.; formal analysis, F.C., O.T.Y; investigation, F.C., O.T.Y, A.E., M.P.; resources, F.C., A.E., M.P.; data curation, F.C., A.E., M.P., T.K.A.; writing—original draft preparation, all authors; writing—review and editing, F.C., M.S.; visualization, F.C.; supervision, M.S.; project administration, F.C.; funding acquisition, F.C.

Funding: This study was organized with project data numbered TSA-2022-4031, supported by Çanakkale Onsekiz Mart University Scientific Research Projects Coordination Unit, and conducted by F.C. This study was organized with project data numbered TSA-2022-4031, supported by Çanakkale Onsekiz Mart University Scientific Research Projects Coordination Unit and conducted by F.C.

Data Availability Statement: Data are available upon request from the corresponding author.

Acknowledgments: We would like to thank Dr. Ruhiye Nilay Tezel for providing the laboratory facilities for the characterization analysis of NPs.

Conflicts of Interest: The authors declare no conflict of interest.

References

1. Chang, T.K.; Abbott, F.S. Oxidative stress as a mechanism of valproic acid-associated hepatotoxicity. *Drug Metabolism Reviews* 2006, 38(4), 627-639. https://doi.org/10.1080/03602530600959433.
2. Tong, V. Investigation of valproic acid-associated oxidative stress and hepatotoxicity. *Doctoral thesis. Doctor of Philosophy Pharmaceutical Sciences.* University of British Columbia, 2005. https://doi.org/10.14288/1.0092257.
3. Hiemke, C.; Bergemann, N.; Clement, H.W.; Conca, A.; Deckert, J.; Domschke, K.; Baumann, P. Consensus guidelines for therapeutic drug monitoring in neuropsychopharmacology: Update 2017. *Pharmacopsychiatry* 2018, 51(01/02), 9-62. https://doi.org/10.1055/s-0043-116492.
4. Tseng, Y.J.; Huang, S.Y.; Kuo, C.H.; Wang, C.Y.; Wang, K.C.; Wu, C.C. Safety range of free valproic acid serum concentration in adult patients. *PLoS One* 2020, 15(9), e0238201, 1-11. https://doi.org/10.1371/journal.pone.0238201.
5. Silva, M.F.B.; Aires, C.C.P.; Luis, P.B.M.; Ruiter, J.P.N.; IJlst, L.; Duran, M.; Tavares de Almeida, I. Valproic acid metabolism and its effects on mitochondrial fatty acid oxidation: A review. *Journal of Inherited Metabolic Disease* 2008, 31(2), 205-216. https://doi.org/10.1007/s10545-008-0841-x.
6. Roy, S.; Rhim, J.W. Fabrication of chitosan-based functional nanocomposite films: Effect of quercetin-loaded chitosan nanoparticles. *Food Hydrocolloids* **2021**, *121*, 107065, 1-11. https://doi.org/10.1016/j.foodhyd.2021.107065.

7. Messias de Souza, G.; Gervasoni, L.F.; Rosa, R.D.S.; de Souza Iacia, M.V.M.; Nai, G.A.; Pereira, V.C.; Winkelstroter, L.K. Quercetin-loaded chitosan nanoparticles as an alternative for controlling bacterial adhesion to urethral catheter. *International Journal of Urology* 2022, 29(10), 1228-1234. https://doi.org/10.1111/iju.14958.
8. Jaiswal, A.; Venkatachalam, S.; De, A.; Namdev, B.; Ramaswamy, R.; Natarajan, J. Preparation, Characterization and Optimization of Repurposed Valproic Acid Loaded Carboxymethyl Chitosan Nanoparticles by Box–Behnken Design for Alzheimer Management. *Indian Journal of Pharmaceutical Education and Research* 2021, 55(1), 75-86. https://doi.org/10.5530/ijper.55.1s.39.
9. Zhang, Y.; Yang, Y.; Tang, K.; Hu. X.; Zou, G. Physicochemical characterization and antioxidant activity of quercetin-loaded chitosan nanoparticles. *Journal of Applied Polymer Science* 2008, 107(2), 891-897. https://doi.org/10.1002/app.26402.
10. Wang, D.; Wang, K.; Liu, Z.; Wang, Z.; Wu, H. Valproic acid-labeled chitosan nanoparticles promote recovery of neuronal injury after spinal cord injury. *Aging (Albany NY)* 2020, 12(10), 8953-8967. https://doi.org/10.18632/aging.103125.
11. Jardim, K.V.; Siqueira, J.L.N.; Báo, S.N.; Parize, A.L. In vitro cytotoxic and antioxidant evaluation of quercetin loaded in ionic cross-linked chitosan nanoparticles. *Journal of Drug Delivery Science and Technology* **2022**, *74*, 103561. https://doi.org/10.1016/j.jddst.2022.103561.
12. Blois, M.S. Antioxidant determinations by the use of a stable free radical. *Nature* 1958, 181(4617), 1199-1200. https://doi.org/10.1038/1811199a0.
13. Re, R.; Pellegrini, N.; Proteggente, A.; Pannala, A.; Yang, M.; Rice-Evans, C. Antioxidant activity applying an improved ABTS radical cation decolorization assay. *Free Radical Biology and Medicine* 1999, 26(9-10), 1231-1237. https://doi.org/10.1016/S0891-5849(98)00315-3.
14. Urkmez, İ.; Çoven, H.İ.K.; Eldem, A.; Pehlivan, M. Anti-Cancer Effects of Trigonella foenum in Neuroblastoma Cell Line. *European Journal of Biology* 2022, 81(2), 251-256. https://doi.org/10.26650/EurJBiol.2022.1167842.
15. Tie, F.; Fu, Y.; Hu, N.; Wang, H. Silibinin protects against H2O2-induced oxidative damage in SH-SY5Y cells by improving mitochondrial function. *Antioxidants* 2022, 11(6), 1101. 1-13 https://doi.org/10.3390/antiox11061101.
16. Subramani, S.E.; Thinakaran, N. Isotherm, kinetic and thermodynamic studies on the adsorption behaviour of textile dyes onto chitosan. *Process Safety and Environmental Protection* **2017**, *106*, 1–10. https://doi.org/10.1016/j.psep.2016.11.024.
17. Liu, D.; Yuan, J.; Li, J.; Zhang, G. Preparation of chitosan poly (methacrylate) composites for adsorption of bromocresol green. *ACS Omega* 2019, 4(7), 12680-12686. https://doi.org/10.1021/acsomega.9b01576.
18. Jantarat, C.; Attakitmongkol, K.; Nichsapa, S.; Sirathanarun, P.; Srivaro, S. Molecularly imprinted bacterial cellulose for sustained-release delivery of quercetin. *Journal of Biomaterials Science, Polymer Edition* 2020, 31(15), 1961-1976. https://doi.org/10.1080/09205063.2020.1787602.
19. Alsarra, I.A.; Al-Omar, M.; Belal, F. Valproic acid and sodium valproate: Comprehensive profile. *Profiles of Drug Substances, Excipients and Related Methodology* **2005**, *32*, 209–240. https://doi.org/10.1016/S0099-5428(05)32008-9.
20. Lopez, T.; Ortiz-Islas, E.; Vinogradova, E.; Manjarrez, J.; Azamar, J.A.; Alvarado-Gil, J.J.; Quintana, P. Structural, optical and vibrational properties of sol–gel titania valproic acid reservoirs. *Optical Materials* 2006, 29(1), 82-87. https://doi.org/10.1016/j.optmat.2006.03.009.
21. Mohammadi, M.; Najavand, S.; Pazhang, M. Immobilization of endoglucanase Cel9A on chitosan nanoparticles leads to its stabilization against organic solvents: The use of polyols to improve the stability. *3 Biotech* **2019**, *9*, 1–10. https://doi.org/10.1007/s13205-019-1794-5.
22. Wangsawangrung, N.; Choipang, C.; Chaiarwut, S.; Ekabutr, P.; Suwantong, O.; Chuysinuan, P.; Techasakul, S.; Supaphol, P. Quercetin/Hydroxypropyl-β-Cyclodextrin Inclusion Complex-Loaded Hydrogels for Accelerated Wound Healing. *Gels* 2022, 8(9), 573, 1-17. https://doi.org/10.3390/gels8090573.
23. Jafarimanesh, M.A.; Ai, J.; Shojaei, S.; Khonakdar, H.A.; Darbemamieh, G.; Shirian, S. Sustained release of valproic acid loaded on chitosan nanoparticles within hybrid of alginate/chitosan hydrogel with/without stem cells in regeneration of spinal cord injury. *Progress in Biomaterials* **2023**, *12*, 75–86. https://doi.org/10.1007/s40204-022-00209-3.
24. Abd El-Rahmanand, S.N.; Suhailah, S. Quercetin nanoparticles: Preparation and characterization. *Indian Journal of Drugs* 2014, 2(3), 96-103. https://www.researchgate.net/publication/309418322.
25. Raj, L.A.; Jonisha, R.; Revathi, B.; Jayalakshmy, E. Preparation and characterization of BSA and chitosan nanopartices for sustainable delivery system for quercetin. *Journal of Applied Pharmaceutical Science* 2015, 5(7), 001-005. https://doi.org/10.7324/JAPS.2015.50701.
26. Li, F.; Jin, H.; Xiao, J.; Yin, X.; Liu, X.; Li, D.; Huang, Q. The simultaneous loading of catechin and quercetin on chitosan-based nanoparticles as effective antioxidant and antibacterial agent. *Food Research International* **2018**, *111*, 351–360. https://doi.org/10.1016/j.foodres.2018.05.038.

27. Ateş, M. Nanoparçacıkların ölçme ve inceleme teknikleri. *Türk Bilimsel Derlemeler Dergisi* 2018, 11(1), 63-69. https://dergipark.org.tr/en/pub/derleme/issue/41668/451254.
28. Zhou, J.; Li, N.; Liu, P.; Liu, Z.; Gao, L.; Jiao, T. Preparation of Fluorescently Labeled Chitosan-Quercetin Drug-Loaded Nanoparticles with Excellent Antibacterial Properties. *Journal of Functional Biomaterials* 2022, 13(3), 141, 1-13. https://doi.org/10.3390/jfb13030141.
29. Baksi, R.; Singh, D.P.; Borse, S.P.; Rana, R.; Sharma, V.; Nivsarkar, M. In vitro and in vivo anticancer efficacy potential of Quercetin loaded polymeric nanoparticles. *Biomedicine & Pharmacotherapy* **2018**, *106*, 1513–1526. https://doi.org/10.1016/j.biopha.2018.07.106.
30. Nathiya, S.; Durga, M.; Devasena, T. Preparation, physico-chemical characterization and biocompatibility evaluation of quercetin loaded chitosan nanoparticles and its novel potential to ameliorate monocrotophos induced toxicity. *Digest Journal of Nanomaterials and Biostructures* **2014**, *9*, 1603–1614. https://www.researchgate.net/publication/279030646.
31. Wu, T.H.; Yen, F.L.; Lin, L.T.; Tsai, T.R.; Lin, C.C.; Cham, T.M. Preparation, physicochemical characterization, and antioxidant effects of quercetin nanoparticles. *International Journal of Pharmaceutics* 2008, 346(1-2), 160-168. https://doi.org/10.1016/j.ijpharm.2007.06.036.
32. Zhang, Y.; Yang, Y.; Tang, K.; Hu, X.; Zou, G. Physicochemical characterization and antioxidant activity of quercetin-loaded chitosan nanoparticles. *Journal of Applied Polymer Science* 2008, 107(2), 891-897. https://doi.org/10.1002/app.26402.
33. Palol, V.V.; Saravana, S.; Subramanyam, V.; Ganapathy, R.; Chinnadurai, R.K.; Subramanian, B. Effects of Valproic Acid with Different Drugs in Ovarian Cancer Cell Lines: An in vitro Study. *Biointerface research in applied chemistry* 2022, 13(3), 1-9. https://doi.org/10.33263/BRIAC133.279.
34. Suematsu, N.; Hosoda, M.; Fujimori, K. Protective effects of quercetin against hydrogen peroxide-induced apoptosis in human neuronal SH-SY5Y cells. *Neuroscience Letters* 2011, 504(3), 223-227. https://doi.org/10.1016/j.neulet.2011.09.028.
35. Manigandan, V.; Nataraj, J.; Karthik, R.; Manivasagam, T.; Saravanan, R.; Thenmozhi, A.J.; Guillemin, G.J. Low molecular weight sulfated chitosan: Neuroprotective effect on rotenone-induced in vitro Parkinson's disease. *Neurotoxicity Research* **2019**, *35*, 505–515. https://doi.org/10.1007/s12640-018-9978-z.
36. Terzioglu Bebitoglu, B.; Oğuz, E.; Acet, G. Effect of valproic acid on oxidative stress parameters of glutamate induced excitotoxicity in SH SY5Y cells. *Experimental and Therapeutic Medicine* 2020, 20(2), 1321-1328. https://doi.org/10.3892/etm.2020.8802.
37. Aluani, D.; Tzankova, V.; Yordanov, Y.; Kondeva-Burdina, M.; Yoncheva, K. In vitro protective effects of encapsulated quercetin in neuronal models of oxidative stress injury. *Biotechnology & Biotechnological Equipment* 2017, 31(5), 1055-1063. https://doi.org/10.1080/13102818.2017.1347523.
38. Xi, J.; Zhang, B.; Luo, F.; Liu, J.; Yang, T. Quercetin protects neuroblastoma SH-SY5Y cells against oxidative stress by inhibiting expression of Krüppel-like factor 4. *Neuroscience Letters* 2012, 527(2), 115-120. https://doi.org/10.1016/j.neulet.2012.08.082.
39. Han, Q.; Wang, X.; Cai, S.; Liu, X.; Zhang, Y.; Yang, L.; Yang, R. Quercetin nanoparticles with enhanced bioavailability as multifunctional agents toward amyloid induced neurotoxicity. *Journal of Materials Chemistry B* 2018, 6(9), 1387-1393. https://doi.org/10.1039/c7tb03053c.
40. Teleanu, D.M.; Chircov, C.; Grumezescu, A.M.; Volceanov, A.; Teleanu, R.I. Impact of nanoparticles on brain health: An up to date overview. *Journal of Clinical Medicine* 2018, 7(12), 490, 1-14. https://doi.org/10.3390/jcm7120490.